

TeachingBot: Robot Teacher for Human Handwriting

Zhimin Hou^{2*}, Cunjun Yu^{1*}, David Hsu^{1,3}, Haoyong Yu²

Abstract—Teaching physical skills to humans requires one-on-one interaction between the teacher and the learner. With a shortage of human teachers, such a teaching mode faces the challenge of scaling up. Robots, with their replicable nature and physical capabilities, offer a solution. In this work, we present TeachingBot, a robotic system designed for teaching handwriting to human learners. We tackle two primary challenges in this teaching task: the adaptation to each learner’s unique style and the creation of an engaging learning experience. TeachingBot captures the learner’s style using a probabilistic learning approach based on the learner’s handwriting. Then, based on the learned style, it provides physical guidance to human learners with variable impedance to make the learning experience engaging. Results from human-subject experiments based on 15 human subjects support the effectiveness of TeachingBot, demonstrating improved human learning outcomes compared to baseline methods. Additionally, we illustrate how TeachingBot customizes its teaching approach for individual learners, leading to enhanced overall engagement and effectiveness.

I. INTRODUCTION

Robots play a crucial role in various physical interaction tasks with humans [1]. They go beyond being mere learners [2], [3], collaborators [4], or assistant [5], [6] of humans, and have the potential to become the teacher for humans [7]. In human physical skill learning, such as writing characters, physical guidance provides a more direct learning signal than other signals, e.g., visual signal. However, physical guidance often requires personalized one-on-one interactions between the teacher and the learner. With a shortage of human teachers, robots, being highly scalable and capable of physical interaction, can be promising candidates. In this work, we focus on character writing, an essential skill used in daily life. The robot serves as the *teacher* to provide guidance through physical interaction with humans to teach handwriting.

Teaching humans to write effectively presents challenges even for human teachers. First, human learners have different writing styles, leading to different learning preferences. Secondly, striking the right level of guidance is difficult. An insufficient amount of guidance would fail to provide adequate support for human learning, while excessive assistance would result in a dependency on the teacher’s guidance [5], hindering learner’s acquisition of essential skills in the task [7]. Therefore, a successful robot teaching system for writing

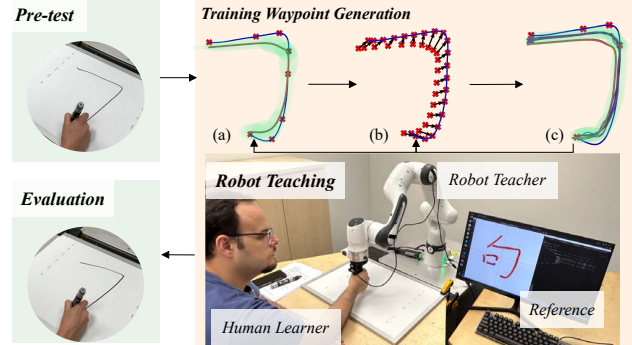


Fig. 1: The pipeline of TeachingBot. It consists of three phases: 1) Pre-test: collects learner handwriting; 2) Robot teaching: (a) captures learner style, (b) generates individual impedance, and (c) generates individual training trajectory for robot; 3) Evaluation: evaluates learner improvement.

must adapt to learner’s style and promote engagement while providing physical guidance.

We present a robot system, illustrated in Fig. 1, referred to as *TeachingBot*, aiming to enable the human learner to follow the physical guidance of the robot teacher to learn to write the reference style of given Chinese characters. TeachingBot can capture learner’s style from its handwriting and provide necessary physical guidance to learners by two main steps. First, the robot collects handwriting of the human learner. The dispersion of the writing trajectories represents the style of the learner for writing the given reference character. Particularly, inspired by [8], we apply the mixture of Gaussian distributions to encode the learner’s styles by the mean trajectory and its variability. Then, leveraging the learned learner’s styles and the reference style, we use the probabilistic learning method to generate the teaching trajectory for the robot teacher. Second, utilizing the generated teaching trajectory, the robot engages in compliant interactions with the human learner using variable impedance control [9]. In order to offer well-balanced guidance to each learner, the impedance should be increased when the learner deviates significantly from the reference and reduces impedance to encourage the learner’s engagement when the deviation is minor [5], [10], [11]. This integration allows TeachingBot to encode learner styles into adaptive physical guidance, thus, TeachingBot can generate physical guidance that tailored to an individual learner. As a result, TeachingBot provides physical guidance that does not impede individual expression and facilitates effective learning.

In this work, it’s crucial to distinguish between robot learning and robot teaching. Robot learning involves robots acquiring skills or knowledge to enhance their capabilities, while robot teaching positions the robot as an instructor guiding human learners, as exemplified by TeachingBot.

* Authors have contributed equally, and names are in alphabetical order. The authors are associated with the ¹School of Computing, ²Department of Biomedical Engineering, ³Smart Systems Institute, National University of Singapore.

In Section IV, all subjects gave informed consent and testing was approved by National University of Singapore Institutional Review Board (NUS-IRB-2022-216).

Through human subject experiments involving various Chinese characters, we demonstrate the effectiveness of TeachingBot in facilitating human learning and illustrate how it customizes its teaching approach for individual learners, thereby enhancing overall engagement in human learning. The potential of robot teaching opens up new opportunities for scaling up education and offering learning opportunities to many, even in the absence of human teachers.

II. RELATED WORK

Teaching Algorithm: Various algorithms have been employed for human learning, with successes in crowd classification and concept acquisition [12], [13], [14], [15]. However, mastering intricate motor control skills through mere visual or verbal cues remains challenging. Recent advancements integrate skill discovery techniques from reinforcement learning to establish curricula based on skill decomposition, enhancing human motor skill acquisition [16]. The emergence of advanced language models has introduced language correction as a tool to facilitate human learning [17]. In the realm of robot-assisted learning, the concept of robot teaching has emerged. Robots can facilitate human learning physically by using specified dynamics [7], [18], [19]. In our work, instead of only providing physical guidance, we aim to achieve adaptive teaching by learning the style of the learner in the physical guide for teaching.

Robot Training Strategies: Extensive research has explored encoding human skills and representing robot skills [2]. Probabilistic methods like Gaussian Mixture Model (GMM)/Gaussian Mixture Regression (GMR) and Dynamic Movement Primitives (DMP) [20], [21], [22] have succeeded in generating robot reference trajectories. Others, such as Probabilistic DMP (ProMP) and Gaussian Process (GP) models [23], [8], [3], have utilized basis functions for trajectory representation and adaptation. While these methods have been applied in physical human-robot interaction (pHRI) tasks like robotic training and rehabilitation [24], [25], most of them focus on robots learning from human experts. In contrast, our framework is centered on generating appropriate trajectories for human learning.

Furthermore, varying the intensity of interaction is crucial for effective human learning [26]. Active engagement of human users can enhance neural plasticity and accelerate learning [27], [5]. Variable stiffness/impedance controllers are highly effective for modulating physical interaction [28], [10]. They adapt assistance levels by updating impedance parameters, as seen in [9], [29], [11], where time-varying impedance is iteratively adjusted based on motion tracking errors. LfDs and reinforcement learning (RL) methods were also developed to achieve state-varying modulation for physical interaction based on task goals and human user characteristics [30], [31], [32]. However, model-free RL faces challenges in pHRI tasks due to high sample complexity [31], [32]. In contrast, TeachingBot, proposes a variable impedance scheme to efficiently facilitate human learning by adjusting teaching intensity based on the learner’s style and real-time writing performance.

III. METHOD

A. Problem Formulation

We build upon prior work [7] where the target task is a Markov Decision Process (MDP). and the teaching task is a Partially Observable Markov Decision Process (POMDP). The target task is to write Chinese characters and the teaching task is to teach human such skill. The teaching policy is designed to influence the learner’s performance through interactive actions, such as generating reference character trajectories and introducing physical interaction impedance to enrich feedback. The goal of the TeachingBot is to efficiently teach the human learner to write the reference character. Specifying the elements within the POMDP is challenging due to the absence of an accurate human learning model. Instead of solving the complete POMDP, we choose a simplified solution. TeachingBot adapts support to the learner’s needs purely based on the current observation of the learner’s style and performance, which is practical in scenarios with limited knowledge of human learning dynamics [16], [33].

B. Overview of TeachingBot

The overview of TeachingBot is depicted in Fig. 2. The reference character is denoted by a variable $c \in \mathcal{C}$, represented by an image. \mathcal{C} is the dataset including the images of reference Chinese characters. To facilitate the robot teaching trajectory generation, the reference waypoints $\{\chi_c^n\}_{n=1}^N$ of each stroke are extracted from the image of the reference character. For instance, the reference waypoints of two strokes are plotted in Fig. 2(a). As illustrated in Fig. 1, the human learner would grasp the robot’s handle, and the robot teacher guides the human learner to write the reference character by following a generated reference trajectory. For one round of finishing writing the character, we call it one *teaching iteration*. A variable impedance controller (VIC) is implemented with the sample interval T_s to provide correction following the given reference trajectory $\tau_d = [\mathbf{x}_d(0), \mathbf{x}_d(T_s), \dots, \mathbf{x}_d(\Delta t_c)]$, $\mathbf{x}_d \in \mathbb{R}^3$ is the reference position of the robot end-effector. Particularly, at each robot teaching iteration, a reference trajectory is generated for the robot teacher. The actual writing trajectory and interaction force trajectory are respectively collected as $\tau = [\mathbf{x}(0), \mathbf{x}(T_s), \dots, \mathbf{x}(\Delta t_c)]$ and $\Gamma = [\mathbf{F}_h(0), \mathbf{F}_h(T_s), \dots, \mathbf{F}_h(\Delta t_c)]$, $\mathbf{F}_h \in \mathbb{R}^3$ is the interaction force and Δt_c is writing time of the given reference character c . The writing trajectory is also downsampled to N writing waypoints $[\chi(0), \chi(T_w), \dots, \chi(\Delta t_c)]$, T_w is the time interval of the waypoints ($T_s \ll T_w$). The writing waypoints are abbreviated as $\{\chi^n\}_{n=1}^N$ in the following.

Given a reference character c , the robot teaching is repeated for I iterations. At i -th teaching iteration ($i \in I$), the previous L actual writing trajectories are collected as $\{\tau^l\}_{l=1}^L$, which are downsampled to writing waypoints $\{\{\chi^{l,n}\}_{n=1}^N\}_{l=1}^L$ for learner style learning. The dataset $\mathcal{D}_L^i = \{\{t_n^l, \chi^{l,n}\}_{n=1}^N\}_{l=1}^L$ is constructed to include all time-driven waypoints. The key via-points are extracted from the

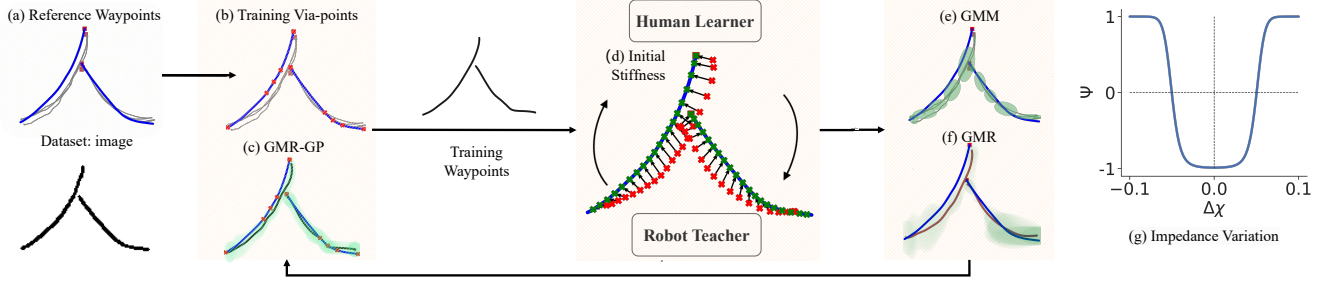


Fig. 2: Overview of TeachingBot. At each teaching iteration, a reference character is selected from the image dataset. The reference and writing waypoints are extracted from the reference writing image and handwritten images of the learner (as depicted by blue and gray lines in (a)). First, a GMM is fitted to capture main features of previous writing waypoints, and GMR is used to represent learner writing styles calculated from the learned GMM (as depicted in (e) and (f)). Second, training via-points are derived from reference waypoints (as depicted by red scatters in (b)). Third, a GMR-GP is fitted to generate training waypoints based on the training via-points and the learned writing style (as depicted by black lines in (c)). Then, the initial stiffness of each learner for impedance control is obtained from the difference between writing waypoints and reference waypoints (as depicted in (d)), and an impedance variation function (as depicted in (g)) is utilized to modulate the level of active participation.

reference waypoints as training via-points and stored in \mathcal{D}_V^i . A GMR-GP model $f(\chi_d|t, \mathcal{D}_L^i, \mathcal{D}_V^i)$ is learned to generate the training waypoints $\{\chi_d^{i,n}\}_{n=1}^N$ based on the given human style and training via-points. Afterward, the training waypoints are interpolated into the reference trajectory τ_d^i for robot impedance control.

C. Learner Style Learning

A GMM with Z components is applied to model the joint distribution of the input time $\xi_i = t \in \mathbb{R}^{d_i}$, and output writing waypoint $\xi_o = \chi \in \mathbb{R}^{d_o}$, as

$$\mathcal{P}(\xi) = \sum_{z=1}^Z h_z \mathcal{N}(\xi; \mu_z, \Sigma_z), \xi = [\xi_i, \xi_o]^T, \quad (1)$$

where h_z , μ_z , and Σ_z are the prior probability, mean, and covariance of the z -th Gaussian component, respectively. These parameters are optimized by the Expectation-Maximization algorithm given the dataset \mathcal{D}_L^i [21], [34], [8]. Therefore, the learner style is represented by a probabilistic reference trajectory $\{\hat{\chi}^n\}_{n=1}^N$. Each waypoint $\hat{\chi}^n$ is retrieved from a conditional Gaussian distribution $\mathcal{P}(\hat{\chi}^n|t_n) = \mathcal{N}(\hat{\mu}(t_n), \hat{\Sigma}(t_n))$. $\hat{\mu}(t_n)$ and $\hat{\Sigma}(t_n)$ are the conditional mean and covariance. The covariance $\hat{\Sigma}(t_n)$ encapsulates the variability of the learner's potential writing trajectories.

For instance, $L = 3$ writing waypoints of reference character c , which are plotted by grey lines in Fig. 2(a) and Fig. 2(b). The GMM ($Z = 8$) is optimized and visualized by the green ellipses in Fig. 2(e). The mean writing waypoints and variance are derived from GMM, which are plotted by the green line and green region in Fig. 2(f).

D. Training Via-points Extraction

We perform curvature-based trajectory compression to extract the training via-points from the reference waypoints. Particularly, we retain waypoints where the curvature (change in direction) is highest, as these waypoints are likely to represent features of the reference character. Given the reference waypoints $[\chi_c^1, \dots, \chi_c^N]$, calculate curvature κ_n for each interior waypoint χ_c^n using the first order derivative $\dot{\chi}_c^n$ and second order derivative $\ddot{\chi}_c^n$. The curvature can be computed as $\kappa_n = \ddot{\chi}_c^n / (1 + (\dot{\chi}_c^n)^2)^{1.5}$. Then, select the H waypoints with the highest curvature values as training via-points, indicating significant changes in trajectory direction.

The extracted training via-points are stored in $\mathcal{D}_V^i = \{t_h^i, \chi_c^h\}_{h=1}^H$ ($H \ll N$). In Fig. 2(b), we visualize the $H = 5$ extracted training via-points by red scatters.

E. Training Waypoints Generation

Multi-output GP (MOGP) is employed to fit the deterministic relationship $\xi_o = f(\xi_i) + \epsilon_t$ from the input $\xi_i = t$ to vector-valued output $\xi_o = \chi$, $\epsilon_t = [\epsilon_t^1, \epsilon_t^p, \dots, \epsilon_t^{d_o}]$, $\epsilon_t^p \sim \mathcal{N}(0, \sigma_p^2)$. The distribution of χ input t is given by $\chi(t) \sim \mathcal{GP}(\mu(t), k(t, t'))$, where $\mu(\cdot) : \mathbb{R}^{d_i} \rightarrow \mathbb{R}^{d_o}$ and $k(\cdot, \cdot) : \mathbb{R}^{d_i} \times \mathbb{R}^{d_i} \rightarrow \mathbb{R}^{d_o} \times \mathbb{R}^{d_o}$ are the mean and kernel function. The joint distribution of observed samples and the predicted output χ^* of the input t_* is given by

$$\begin{bmatrix} \chi^{1:N} \\ \chi^* \end{bmatrix} \sim \mathcal{N} \left(\begin{bmatrix} \mu(t_{1:N}) \\ \mu(t_*) \end{bmatrix}, \begin{bmatrix} \mathbf{K}(t, t) + \Sigma_\epsilon & \mathbf{K}(t, t_*) \\ \mathbf{K}(t_*, t) & \mathbf{K}(t_*, t_*) \end{bmatrix} \right), \quad (2)$$

where $\chi^{1:N}$ are the observed values at input $t_{1:N}$. $\mathbf{K}(t, t) \in \mathbb{R}^{N d_o \times N d_o}$, $\mathbf{K}(t, t_*) \in \mathbb{R}^{N d_o \times d_o}$, $\mathbf{K}(t_*, t) \in \mathbb{R}^{d_o \times N d_o}$, and $\mathbf{K}(t_*, t_*) \in \mathbb{R}^{d_o \times d_o}$ are the Gram matrices that all elements are calculated by the kernel function of all input pairs (t, t) . Similar to [8], [2], the kernel function $k(t, t') = \sum_{q=1}^Q \Xi_q k_q(t, t')$ is designed based on the Linear Model of Coregionalization (LMC) assumption. $\Xi_q \in \mathbb{R}^{d_o \times d_o}$ is a positive semi-definite coregionalization matrix. $k_q(t, t')$ is the scalar kernel function. The design of Ξ_q and $k_q(\cdot, \cdot)$ depends on the prior knowledge of $\mathcal{GP}(\cdot)$.

For i -th teaching iteration, given the previous writing waypoints in \mathcal{D}_L^{i-1} , the posterior distribution of the learner writing waypoints is derived as a multivariate Gaussian distribution (MGD), as $\mathcal{P}(\chi^*|t_*, \mathcal{D}_L^{i-1}) \sim \mathcal{N}(\mu_L^*, \Sigma_L^*)$. The mean and covariance μ_L^* and Σ_L^* are calculated as

$$\begin{aligned} \mu_L^* &= \mu(t_*) + \mathbf{K}(t_*, t)(\mathbf{K}(t, t) + \Sigma_\epsilon)^{-1}(\chi^{1:N} - \mu(t)) \\ \Sigma_L^* &= \mathbf{K}(t_*, t_*) - \mathbf{K}(t_*, t)(\mathbf{K}(t, t) + \Sigma_\epsilon)^{-1}\mathbf{K}(t, t_*), \end{aligned} \quad (3)$$

where Σ_ϵ is the covariance matrix of the given noise. $\mu(t_*)$ is the prior mean value of the input t_* .

The training via-points in \mathcal{D}_V^i are considered as the new observations besides the previous observations of learner styles in \mathcal{D}_L^{i-1} . The style of the learner has been fitted by GMR from \mathcal{D}_L^{i-1} in Section III-C. Unlike standard MOGP, GMR-GP model replaces the prior mean value $\mu(t_*)$ with the estimated GMR mean value. The kernel function

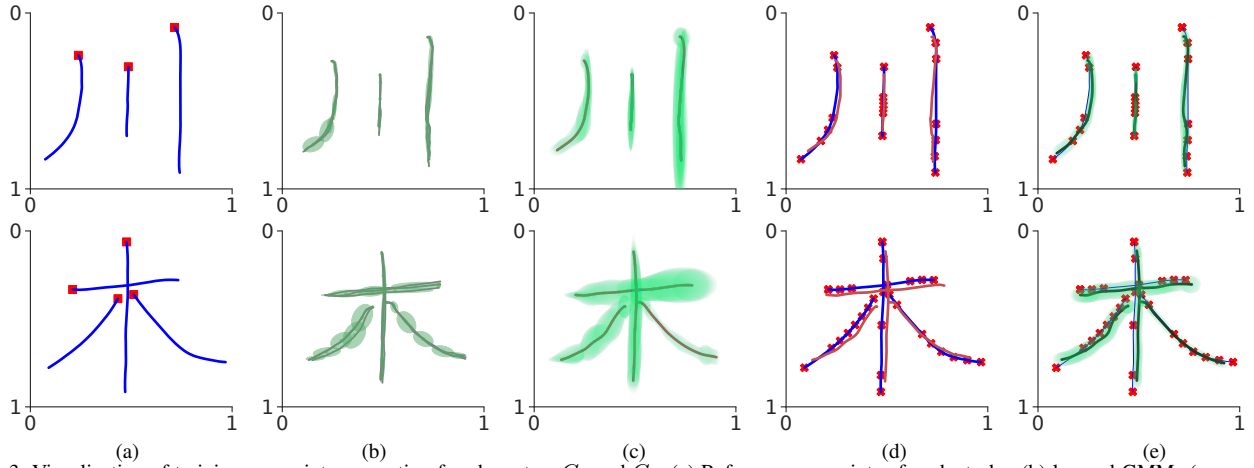


Fig. 3: Visualization of training waypoints generation for characters C_3 and C_4 . (a) Reference waypoints of each stroke; (b) learned GMMs (green ellipse) from writing waypoints; (c) learned style by GMR from writing waypoints; (d) training via-points; (e) generated training waypoints (black lines) by GMR-GP.

$\mathbf{k}(t, t') = \sum_{z=1}^Z h_z(t)h_z(t')\widehat{\Sigma}_z\mathbf{k}_z(t, t')$ is designed based on the learned variability. $h_c(t)$ and $\widehat{\Sigma}_z$ are the derived responsibilities and componentwise conditional covariance matrix calculated by (1). The MGD for the training waypoints generation is rewritten as

$$\begin{aligned} \mathcal{P}(\mathcal{X}^*|t_*, \mathcal{D}_L^{i-1}, \mathcal{D}_V^i) &\propto \mathcal{P}(\mathcal{X}^*|t_*, \mathcal{D}_L^{i-1})\mathcal{P}(\mathcal{X}^*|t_*, \mathcal{D}_V^i), \\ \mathcal{P}(\mathcal{X}^*|t_*, \mathcal{D}_L^{i-1}, \mathcal{D}_V^i) &\sim \mathcal{N}(\boldsymbol{\mu}_{L-V}^i, \boldsymbol{\Sigma}_{L-V}^i), \end{aligned} \quad (4)$$

where $\boldsymbol{\mu}_{L-V}^i$ and $\boldsymbol{\Sigma}_{L-V}^i$ can be derived based on $\{\boldsymbol{\mu}_L^*, \boldsymbol{\Sigma}_L^*, \boldsymbol{\mu}_V^*, \boldsymbol{\Sigma}_V^*\}$ according to [2]. $\boldsymbol{\mu}_L^*$ and $\boldsymbol{\Sigma}_L^*$ are the mean and covariance of $\mathcal{P}(\mathcal{X}^*|t_*, \mathcal{D}_L^{i-1})$; $\boldsymbol{\mu}_V^*$ and $\boldsymbol{\Sigma}_V^*$ are the mean and covariance of $\mathcal{P}(\mathcal{X}^*|t_*, \mathcal{D}_V^i)$.

Afterwards, the training waypoints $\{\mathcal{X}_d^{i,n}\}_{n=1}^N$ is sampled from the learned posterior distribution in (4) given $\{t_n\}_{n=1}^N$. For instance, we use the Matérn kernel (lengthscale $\nu = 2.5$) for above \mathcal{GP} fitting. Given the training via-points in Fig. 2(b) and learned styles in Fig. 2(e), the sampled training waypoints are plotted by the black line in Fig. 2(c).

F. Variable Impedance Control

The reference trajectory $\boldsymbol{\tau}^i$ for the robot control is obtained by interpolating the obtained training waypoints $\{\mathcal{X}_d^{i,n}\}_{n=1}^N$. At each actuation step, the control input \mathbf{u} is sampled from the controller $\pi(\mathbf{u}|\mathbf{x}; \mathbf{x}_d, \mathcal{K}_d^i, \mathcal{B}_d^i)$ for the reference motion tracking. $\mathcal{K}_d^i \in \mathbb{R}^{3 \times 3}$ and $\mathcal{B}_d^i \in \mathbb{R}^{3 \times 3}$ are the reference stiffness and damping for i -th teaching iteration.

1) *Control Law*: A control law is designed as $\mathbf{u} = \mathbf{J}^T [-\mathcal{K}_d^i(\mathbf{x} - \mathbf{x}_d) - \mathcal{B}_d^i(\dot{\mathbf{x}} - \dot{\mathbf{x}}_d) + \mathbf{F}_{fd}]$, where $\dot{\mathbf{x}}$ and $\dot{\mathbf{x}}_d$ are the actual velocity and the reference velocity. \mathbf{J} is the Jacobian matrix. Similar to [35], \mathbf{F}_{fd} is added to compensate for the robot dynamics.

2) *Impedance Variation*: For each learner and given the reference character c , \mathcal{K}_d^i and \mathcal{B}_d^i are updated as follows $\mathcal{K}_d^i = \mathcal{K}_r + \mathcal{K}_s^i$, $\mathcal{B}_d^i = \mathcal{B}_r + \mathcal{B}_s^i$, where \mathcal{K}_r and \mathcal{B}_r are the initial stiffness and damping based on the individual pre-test without robot teaching. \mathcal{K}_s^i and \mathcal{B}_s^i are updated according to the $(i-1)$ -th training performance to adjust the engagement of the learner. \mathcal{K}_s^0 and \mathcal{B}_s^0 for the first teaching iteration are set to zero.

L writing images for the reference character c during individual pre-test are collected as $\{\tilde{c}_l\}_{l=0}^L$. The writing waypoints are extracted as $\{\{\mathcal{X}_{\tilde{c}_l}^{l,n}\}_{n=1}^N\}_{l=1}^L$. The mean writing waypoints $\bar{\mathcal{X}}_c$ can be estimated following Section III-C. \mathcal{X}_c and $\bar{\mathcal{X}}_c$ are aligned by the Dynamic Time Warping (DTW)[36], as depicted in Fig. 2(d). \mathcal{K}_r is obtained as follows

$$\mathcal{K}_r = \beta_r |\Delta \bar{\mathcal{X}}|, \Delta \bar{\mathcal{X}} = \bar{\mathcal{X}}_c - \mathcal{X}_c, \quad (5)$$

where β_r is the coefficient. In practice, damping \mathcal{B}_r is obtained from the stiffness $\mathcal{B}_r = 1/2\sqrt{\mathcal{K}_r}$. \mathcal{K}_s^i and \mathcal{B}_s^i are obtained as

$$\begin{aligned} \mathcal{K}_s^i &= \mathcal{K}_s^{i-1} + \beta_{\mathcal{K}} \Psi(\Delta \mathcal{X}^{i-1}), \mathcal{B}_s^i = 1/2\sqrt{\mathcal{K}_s^i}, \\ \Psi(\Delta \mathcal{X}^{i-1,p}) &= \frac{\exp(\alpha \Omega^{i-1,p} - \Pi_p) - 1}{\exp(\alpha \Omega^{i-1,p} - \Pi_p) + 1}, p = 0, 1, 2, \end{aligned} \quad (6)$$

where $\Psi(\cdot)$ is an element-wise scalar function (as shown in Fig. 2(g)). $\Delta \mathcal{X}^{i-1} = \mathcal{X}^{i-1} - \mathcal{X}_d^{i-1}$ and $\Delta \mathcal{X}^{i-1,p}$ is p -th element of $\Delta \mathcal{X}^{i-1}$. $\Omega^{i-1,p} = \Delta^2 \mathcal{X}^{i-1,p} - \Pi_p^2$. $\beta_{\mathcal{K}}$ is the coefficient to regulate the convergence speed. Π_p is the predefined threshold that determines the region whether to increase the assistance to the learner. α is a positive scalar.

IV. EXPERIMENTS

We conduct human-subject experiments to answer the following questions: 1) In general, does TeachingBot enable humans to learn the target skill more efficiently compared with baselines?; 2) Is TeachingBot able to capture human style and provide adaptive guidance to learners?; and 3) Is the learning experience with TeachingBot encouraging to the learner?

A. Experimental Setups

1) *Hardware Setup*: We employ the Franka Emika Panda robot, a 7-DoF torque-controlled robot for all teaching experiments (as depicted in Fig. 1) The length and width of the writing space are 350mm and 350mm, respectively. The interaction force on the end-effector handle is estimated from joint torques. The reference character c is represented by a 128×128 image. During the pre-test and evaluation phases,

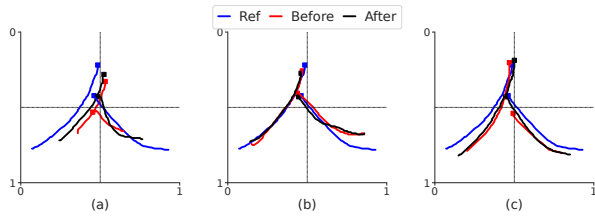


Fig. 4: Writing performance before teaching (red lines) and after teaching (black lines) according to M_1 of character C_2 by three groups. (a) FC; (b) RGW; (c) Ours.

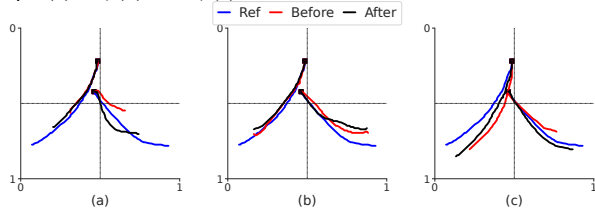


Fig. 5: Writing performance before teaching (red lines) and after teaching (black lines) according to M_2 of character C_2 by three groups. (a) FC; (b) RGW; (c) Ours.

the handwritten characters of human learners are captured by a mounted camera, and the image is also resized to 128×128 . The reference waypoints and writing waypoints of each character are extracted from the images via feature extraction methods. For the robot-teaching phase, the learner’s actual writing trajectories are represented by the actual position of the robot end-effector.

The impedance control of the robot teacher runs at 1000Hz ($T_s = 0.001s$). The maximal stiffness of the VIC is set to $\mathcal{K}_d^{max} = [1200, 1200, 1200]N/m$. All parameters for style learning and waypoints generation are set as $N = 200$, $L = 3$, $H = 5$, and $I = 9$. The parameters for impedance variation are set as $\beta_r = 1000N/m^2$, $\beta_K = 100N/m^2$, $\Pi_p = 0.05m$ and $\alpha = 2000$.

2) *Data Curation*: The Chinese character dataset \mathcal{C} we utilize is obtained from [link](#). We select 5 distinct characters with varying numbers of strokes and levels of complexity from the dataset: C_1 : 一, C_2 : 人, C_3 : 川, C_4 : 木, and C_5 : 甸, in ascending order of complexity. As depicted in Fig. 3, we visualized the process for generating the training waypoints of characters C_3 and C_4 following the implementation in Section III.

B. Experimental Protocol

Baselines: We assess the effectiveness of TeachingBot by comparing it to two primary baselines:

- 1) *Font-Copy (FC)*: Participants are only allowed to look at the reference character without any physical correction from the robot. The subjects in this group are referred to as *Group 1 (G1)*.
- 2) *Robot Guided Writing (RGW)*: Similarly to robotic physical training [29] and rehabilitation [9], [11], this baseline uses high stiffness \mathcal{K}_d^{max} to fully guide participants in replicating the reference trajectory without impedance variation for considering the learner active engagement. The subjects in this group are referred to as *Group 2 (G2)*.

The group of subjects trained with TeachingBot is referred

TABLE I: Average Similarity Improvement and Interaction Force.

Method	Value(%) M_1	Value(%) M_2	Force (N)
FC	18.790 ± 12.15	17.521 ± 7.621	NA
RGW	25.008 ± 13.044	24.837 ± 5.362	6.813 ± 1.131
Ours	34.296 ± 14.03	36.436 ± 6.986	19.921 ± 4.096

to as *Group 3 (G3)*. We recruited 15 human subjects, with 4 males and 1 female in each group who have different Chinese character writing experience. The experiments for each group are implemented for same times ($I = 9$) and consists of three phases:

- 1) *Pre-test*: The pre-test phase occurs before any training to assess the initial performance of each subject, eliminating the influence of prior knowledge. Human subjects write the given reference character L times without any physical guidance or visual guidance. The individual writing time Δt_c of each reference character c is estimated for each subject.
- 2) *Robot Teaching/Font Copy*: For $G2$ and $G3$, as illustrated in Fig. 1, during the robot teaching phase, the learner holds the handle and looks at the actual writing trajectories, and the robot executes the teaching trajectory to guide the learner. The subjects of $G1$ first look at the simulation of character writing on the screen and then handwrite the reference character.
- 3) *Evaluation*: The evaluation phase is conducted after the robot teaching or font copy phase. All subjects are allowed to write the reference character without any reference.

C. Experimental Results

1) *Performance Comparison*: Two key metrics are defined to measure the similarity between the reference and written waypoints using DTW distance[36]. First, as illustrated in Fig. 4, *Metric 1* (M_1) aims to capture the global structural similarity so that the center of the written and reference character are aligned before DTW distance calculation. Second, as illustrated in Fig. 5, unlike M_1 , *Metric 2* (M_2) aims to capture the stroke-wise similarity so that the starting points of reference and written strokes are aligned before DTW distance calculation.

The statistical results of all experiments are presented in Fig. 6. Our first finding is that all subjects of three groups have highly similar initial performance. The average value of the percentage of similarity improvement over all subjects of each group after training is calculated for each character and depicted in Fig. 6(a) and (b). In particular, the average improvement in similarity between M_1 and M_2 of each group over five characters is given in Table I. Compared to both baselines (FC and RGW), it was observed that the improvement of the learners trained with TeachingBot was significantly better. Although, in terms of M_1 , the improvement compared to baselines is not entirely significant ($p < 0.05$) and ($p \approx 0.09$). Compared to RGW, as the M_1 metric focuses on structural similarity, the effect of adaptation to the specific human learning style is marginally significant. That said, this also highlights the importance of physical guidance for teaching learners to write. In terms of

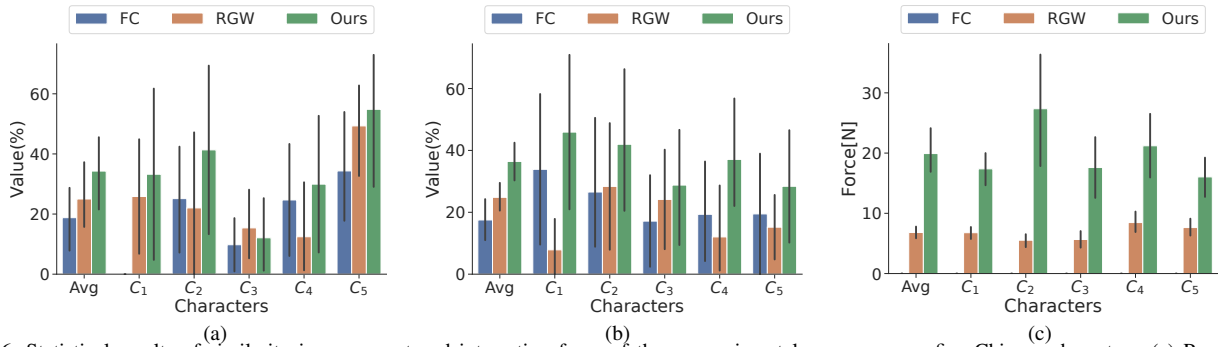


Fig. 6: Statistical results of similarity improvement and interaction force of three experimental groups across five Chinese characters. (a) Percentage of similarity improvement based on M_1 ; (b) percentage of similarity improvement based on M_2 ; (c) average interaction force per waypoint.

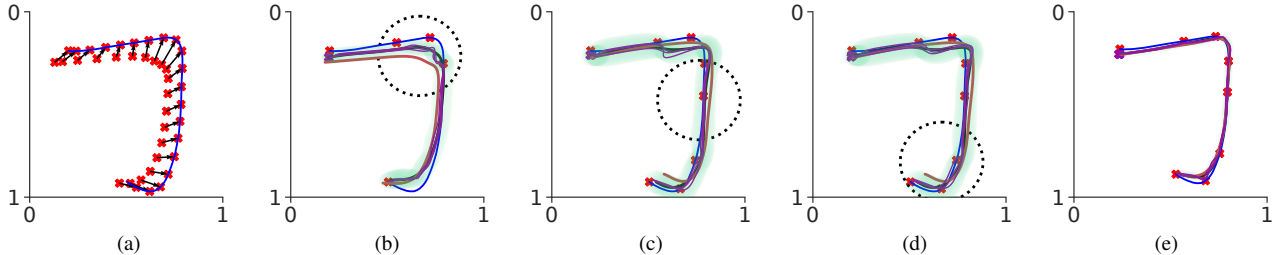


Fig. 7: Visualization of training waypoints changes. Blues lines are reference waypoints, scatter red points are training via-points, red lines are learned means of writing waypoints, black lines are the mean of training waypoints, and purple lines are three sampled potential writing waypoints. (a) Initial reference stiffness generation; (b) 1-st teaching iteration; (c) 3-rd teaching iteration; (d) 6-th teaching iteration; (e) 9-th teaching iteration.

M_2 , in contrast to FC and RGW, TeachingBot leads to better improvement ($p < 0.05$) and ($p < 0.05$). This indicates the need for adaptation when learning fine-grained stroke-wise details of the reference character.

2) *Adaptiveness of Training Waypoints*: In Fig. 7, we visualize the training waypoints of the second stroke of character C_5 for the second subject in G_3 during roboting teaching phase to demonstrate the adaptation ability. In Fig. 7(a), red scatters are the mean of writing waypoints learned from the collected data in pre-test phase. We can see a big difference with the reference waypoints that are plotted by the blue line. The difference is applied to generate the initial reference stiffness. Fig. 7(b), Fig. 7(c), Fig. 7(d), and Fig. 7(e) demonstrate the results of 1-st, 3-rd, 6-th, and 9-th teaching iteration, respectively. In Fig. 7(b), training via-points ($H = 5$) are extracted to enable the learner to capture the curvature of the reference style in the dashed circle. At 3-rd and 6-th teaching iterations, as illustrated in Fig. 7(c) and (d), training via-points ($H = 8$) are extracted to enable the learner to focus on different parts of reference style (as shown in the dashed circles). As the robot teaching progresses, the generated training waypoints are gradually getting closer to the reference waypoints. Particularly, from Fig. 7(d), we can see that the learner can write the reference character with small variability.

3) *Engagement of Human Learners*: As depicted in Fig. 6(a) and Fig. 6(b), learners in G_3 show greater similarity improvement compared to those in G_2 . To validate the learner engagement is crucial for writing skill learning, one indicator of engagement is the interaction force exerted by the learner. A greater force suggests the greater active participation. We calculate the average interaction force for each character across all learners. As depicted in Fig. 6(c), the interaction force in G_3 significantly surpasses that in

G_2 ($p < 0.05$), indicating higher human engagement during robot teaching, which aids in improving writing skills. In this article, we select the same parameters for impedance variation function, which can also be optimized for each learner to achieve higher learning efficiency.

D. Limitations and Discussion

We execute post-experiment survey to assess perceived improvement of human learners' in writing skills. Despite G_3 showing quantitative performance advantages, learners do not report increased confidence in better writing skills compared with G_2 , consistent with previous research [18]. This contradiction leads to two hypotheses: 1) Lack of visual signal integration: human learners may need clear visual signals in addition to physical ones for better understanding. 2) Failure to emulate human instructors: due to differences in morphology and the challenge of replicating real teaching scenarios, full emulation is difficult. These hypotheses guide future robot teaching system development, emphasizing the importance of multi-modal signals (e.g., language and visual) for greater effectiveness and generality.

V. CONCLUSION

In this work, we introduce TeachingBot, a robot teaching system in which robots assume the role of instructors, guiding humans in character writing through adaptive physical interactions. Results from human-subject experiments demonstrate the effectiveness of TeachingBot. Moreover, we provide evidence of how TeachingBot customizes its teaching approach to meet the unique needs of individual learners, leading to enhanced overall engagement and effectiveness. The potential of robot teaching presents exciting opportunities for scaling up education and providing learning opportunities to many, even in the absence of human teachers.

REFERENCES

- [1] D. P. Losey, C. G. McDonald, E. Battaglia, and M. K. O'Malley, "A review of intent detection, arbitration, and communication aspects of shared control for physical human-robot interaction," *Applied Mechanics Reviews*, 2018.
- [2] M. Arduengo, A. Colomé, J. Borràs, L. Sentis, and C. Torras, "Task-adaptive robot learning from demonstration with gaussian process models under replication," *IEEE Robotics and Automation Letters*, 2021.
- [3] Y. Zhou, J. Gao, and T. Asfour, "Learning via-point movement primitives with inter-and extrapolation capabilities," in *2019 IEEE/RSJ International Conference on Intelligent Robots and Systems (IROS)*, 2019.
- [4] Y. Li, K. P. Tee, W. L. Chan, R. Yan, Y. Chua, and D. K. Limbu, "Continuous role adaptation for human-robot shared control," *IEEE Transactions on Robotics*, vol. 31, no. 3, pp. 672–681, 2015.
- [5] A. U. Pehlivan, D. P. Losey, and M. K. O'Malley, "Minimal assist-as-needed controller for upper limb robotic rehabilitation," *IEEE Transactions on Robotics*, 2015.
- [6] D. P. Losey, H. J. Jeon, M. Li, K. Srinivasan, A. Mandlekar, A. Garg, J. Bohg, and D. Sadigh, "Learning latent actions to control assistive robots," *Autonomous robots*, vol. 46, no. 1, pp. 115–147, 2022.
- [7] C. Yu, Y. Xu, L. Li, and D. Hsu, "Coach: Cooperative robot teaching," in *Proceedings of The 6th Conference on Robot Learning*, 2023.
- [8] N. Jaquier, D. Ginsbourger, and S. Calinon, "Learning from demonstration with model-based gaussian process," in *Conference on Robot Learning*, 2020.
- [9] X. Li, Y.-H. Liu, and H. Yu, "Iterative learning impedance control for rehabilitation robots driven by series elastic actuators," *Automatica*, 2018.
- [10] L. Pezeshki, H. Sadeghian, M. Keshmiri, X. Chen, and S. Haddadin, "Cooperative assist-as-needed control for robotic rehabilitation: A two-player game approach," *IEEE Robotics and Automation Letters*, vol. 8, no. 5, pp. 2852–2859, 2023.
- [11] Z. Yang, S. Guo, Y. Liu, M. Kawanishi, and H. Hirata, "A task performance-based semg-driven variable stiffness control strategy for upper limb bilateral rehabilitation system," *IEEE/ASME Transactions on Mechatronics*, 2022.
- [12] A. Singla, I. Bogunovic, G. Bartók, A. Karbasi, and A. Krause, "Near-optimally teaching the crowd to classify," *International Conference on Machine Learning*, 2014.
- [13] S. Zilles, S. Lange, R. Holte, and M. Zinkevich, "Models of cooperative teaching and learning," *Journal of Machine Learning Research*, 2011.
- [14] T. Doliwa, H. U. Simon, and S. Zilles, "Recursive teaching dimension, learning complexity, and maximum classes," *Lecture Notes in Computer Science (including subseries Lecture Notes in Artificial Intelligence and Lecture Notes in Bioinformatics)*, 2010.
- [15] O. Mac Aodha, S. Su, Y. Chen, P. Perona, and Y. Yue, "Teaching categories to human learners with visual explanations," in *IEEE Conference on Computer Vision and Pattern Recognition*, 2018.
- [16] M. Srivastava, E. Biyik, S. Mirchandani, N. Goodman, and D. Sadigh, "Assistive teaching of motor control tasks to humans," in *Advances in Neural Information Processing Systems*, 2022.
- [17] M. Srivastava, N. Goodman, and D. Sadigh, "Generating language corrections for teaching physical control tasks," in *40th International Conference on Machine Learning (ICML)*, 2023.
- [18] R. Tian, M. Tomizuka, A. D. Dragan, and A. V. Bajcsy, "Towards modeling and influencing the dynamics of human learning," *Proceedings of the 2023 ACM/IEEE International Conference on Human-Robot Interaction*, 2023.
- [19] A. N. Rafferty, E. Brunskill, T. L. Griffiths, and P. Shafto, "Faster teaching by pomdp planning," in *Artificial Intelligence in Education*, 2011.
- [20] Y. Huang, J. Silvério, L. Rozo, and D. G. Caldwell, "Generalized task-parameterized skill learning," in *2018 IEEE international conference on robotics and automation (ICRA)*. IEEE, 2018, pp. 5667–5474.
- [21] Y. Huang, L. Rozo, J. Silvério, and D. G. Caldwell, "Kernelized movement primitives," *The International Journal of Robotics Research*, 2019.
- [22] P. Pastor, H. Hoffmann, T. Asfour, and S. Schaal, "Learning and generalization of motor skills by learning from demonstration," in *2009 IEEE International Conference on Robotics and Automation*, 2009.
- [23] A. Paraschos, C. Daniel, J. Peters, and G. Neumann, "Using probabilistic movement primitives in robotics," *Autonomous Robots*, 2018.
- [24] C. Zou, R. Huang, H. Cheng, and J. Qiu, "Learning gait models with varying walking speeds," *IEEE Robotics and Automation Letters*, 2020.
- [25] H. Wu, Z. Xu, W. Yan, Y. Ou, Z. Liao, and X. Zhou, "A framework of rehabilitation-assisted robot skill representation, learning, and modulation via manifold-mappings and gaussian processes," in *2022 IEEE/RSJ International Conference on Intelligent Robots and Systems (IROS)*, 2022.
- [26] M. Sharifi, A. Zakerimanesh, J. K. Mehr, A. Torabi, V. K. Mushahwar, and M. Tavakoli, "Impedance variation and learning strategies in human-robot interaction," *IEEE Transactions on Cybernetics*, 2021.
- [27] Z. Warraich and J. A. Kleim, "Neural plasticity: the biological substrate for neurorehabilitation," *Pm&r*, 2010.
- [28] E. Caldarelli, A. Colomé, and C. Torras, "Perturbation-based stiffness inference in variable impedance control," *IEEE Robotics and Automation Letters*, vol. 7, no. 4, pp. 8823–8830, 2022.
- [29] Y. Li, X. Zhou, J. Zhong, and X. Li, "Robotic impedance learning for robot-assisted physical training," *Frontiers in Robotics and AI*, 2019.
- [30] M. Maaref, A. Rezazadeh, K. Shamaei, R. Ocampo, and T. Mahdi, "A bicycle cranking model for assist-as-needed robotic rehabilitation therapy using learning from demonstration," *IEEE Robotics and Automation Letters*, vol. 1, no. 2, pp. 653–660, 2016.
- [31] S. Pareek, H. J. Nisar, and T. Kesavadas, "Ar3n: A reinforcement learning-based assist-as-needed controller for robotic rehabilitation," *IEEE Robotics & Automation Magazine*, 2023.
- [32] Z. Hou, W. Yang, R. Chen, P. Feng, and J. Xu, "A hierarchical compliance-based contextual policy search for robotic manipulation tasks with multiple objectives," *IEEE Transactions on Industrial Informatics*, vol. 19, no. 4, pp. 5444–5455, 2022.
- [33] B. Clement, D. Roy, P.-Y. Oudeyer, and M. Lopes, "Multi-armed bandits for intelligent tutoring systems," in *Journal of Educational Data Mining*, 2015.
- [34] Y. Huang, F. J. Abu-Dakka, J. Silvério, and D. G. Caldwell, "Toward orientation learning and adaptation in cartesian space," *IEEE Transactions on Robotics*, 2020.
- [35] X. Zhang, L. Sun, Z. Kuang, and M. Tomizuka, "Learning variable impedance control via inverse reinforcement learning for force-related tasks," *IEEE Robotics and Automation Letters*, 2021.
- [36] S. Hu, R. Mendonca, M. J. Johnson, and K. J. Kuchenbecker, "Robotics for occupational therapy: Learning upper-limb exercises from demonstrations," *IEEE Robotics and Automation Letters*, 2021.